Chemical Engineering Science 292 (2024) 119949

Contents lists available at ScienceDirect

Chemical Engineering Science

journal homepage: www.elsevier.com/locate/ces

# Theoretical analysis of gas–liquid mass transfer in Taylor flow capillary reactors

Sergio Bordel [a,b], Norbertus J. R. Kraakman [a,b], Raúl Muñoz [a,b,*]

[a] Institute of Sustainable Processes, University of Valladolid, Dr. Mergelina s/n., Valladolid 47011, Spain
[b] Department of Chemical Engineering and Environmental Technology, University of Valladolid, Dr. Mergelina s/n., Valladolid 47011, Spain

ARTICLE INFO

*Keywords:*
Capillary Reactor
Gas Liquid Mass Transfer
Methane
Modelling
Taylor Flow
Theoretical Analysis

ABSTRACT

Mass transfer in Taylor flow columns was herein investigated from a theoretical point of view. For the first time, an exact solution of the Navier-Stokes equations in the liquid slugs that separate Taylor bubbles has been obtained, as along with a solution for the diffusion equation in the proximity of the hemispherical caps of Taylor bubbles. In addition, an exact solution of the diffusion equation in the liquid films that divide the gas bubbles from the walls of the capillary channel has been obtained. This allows predicting mass transfer rates in Taylor flow capillary reactors using only physical properties (without fitted parameters). The results for a methane-water system were consistent with data from the literature. The contribution of the hemispherical caps was shown to be two orders of magnitude smaller than the contribution of the liquid film flowing around the gas bubbles.

## 1. Introduction

Over the last decades, chemical and biocatalytic reactors operated under Taylor flow regime conditions have attracted an increasing attention due to the high gas–liquid mass transfer rates characteristic of these systems with relatively minimal energy input requirements. The hydrodynamics of gas–liquid flow in capillary channels have been extensively studied within the context of chemical reaction engineering (Nijhuis et al., 2001; Kreutzer et al., 2005; Shao et al., 2009). Capillary reactors using Taylor flow are increasingly being used in industrial processes due to these unique hydrodynamic characteristics and examples of study areas and applications include chemical processing where for example no back-mixing is desired, micro devices (e.g., lab-on-a-chip applications), compact heat exchangers (e.g., printed circuit cooling systems) or to intensify chemical and biocatalytic processes (Haase et al., 2016; Kreutzer et al., 2005).

Gas-liquid mass transfer is expected to have a growing economic impact due to the development of gas-phase biorefineries. The thermal or biological gasification of organic wastes, coupled to the conversion of the generated gas (synthesis gas composed of CO, $H_2$ and $CO_2$ or biogas composed of $CH_4$ and $CO_2$) into bio-based products, represents an innovative alternative to conventional biorefineries. This novel gas-phase biorefineries will allow the upgrading into bio-based chemicals, fuels and materials of the 200, 8.7 and 225 Mt of lignocellulosic waste, sludge from wastewater treatment and municipal solid waste (MSW), respectively, generated annually in the EU (EU Biorefinery Outlook to 2030, 2022). Chemical differences among organic wastes are virtually eliminated in the thermal or biological gasification process. Thus, even organic feedstocks that are toxic or recalcitrant to biological degradation can be converted to CO, $H_2$ and $CO_2$ gas mixtures first, which can be further transformed into commercial products.

The biological conversion of synthesis gas or biogas into added value bioproducts is mediated by the biocatalytic action of bacteria and occurs at room pressure and temperature in gas-phase bioreactors. However, the bioconversion of $CH_4$, CO and $H_2$ is limited by their mass transfer from the gas to the aqueous phase, which requires the development of a new generation of gas-phase bioreactors (Gavala et al., 2021).

In addition, bioprocesses for air quality control have gained acceptance over the last several decades as they have shown in many applications to be sustainable and cost-effective alternatives to conventional physical or chemical technologies. Nevertheless, current biological air pollution control techniques are hampered by their relative inability to treat hydrophobic pollutants (Kraakman et al., 2011). This currently limits their optimization in existing fields such as industrial waste gas abatement, improving indoor air quality and the treatment of dilute off-gases containing the greenhouse gas (GHG) methane (Stone et al., 2017). Biological mitigation of methane emissions is conceivable but

* Corresponding author.
*E-mail address:* sergio.bordel@uva.es (R. Muñoz).

https://doi.org/10.1016/j.ces.2024.119949
Received 24 October 2023; Received in revised form 9 February 2024; Accepted 26 February 2024
Available online 29 February 2024

**Nomenclature**

| | |
|---|---|
| c | the concentration of diffuse species in the liquid |
| $c_0$ | the concentration of diffuse species in the liquid bulk |
| $c_{eq}$ | the concentration of the diffused species in the liquid at equilibrium with the concentration in the gas |
| Ca | capillarity number (-) |
| D | diffusion coefficient ($m^2/s$) |
| $L_b$ | gas bubble length (m) |
| $L_s$ | liquid slug length (m) |
| $L_u$ | total unit length (the sum of both the gas and liquid length) (m) |
| $R_B$ | radius of the backward sides of the bubble (m) |
| $R_F$ | radius of the frontward sides of the bubble (m) |
| $R_c$ | radius of the capillary channel (m) |
| $U_b$ | bubble velocity (m/s) |
| $U_s$ | superficial velocity (m/s) |
| $Q_f$ | volumetric liquid flow in the liquid film along the gas bubble ($m^3$) |
| $V_s$ | the volume of the liquid slug ($m^3$) |
| *Greek letters* | |
| μ | liquid viscosity ($N{\cdot}s/m^2$) |
| σ | surface tension (N/m) |
| ε | gas holdup (-) |
| $\delta_b$ | thickness of the liquid film in the gas bubble region (m) |
| $\delta_c$ | thickness of the liquid film in the liquid slug region (m) |

requires large gas contact times in a bioreactor, while recent studies pointed to the urgency of short-term climate benefits by mitigating methane emissions (Harmsen et al., 2019).

Taylor flow is characterized by elongated gas bubbles separated by liquid slugs. The hydrodynamics of these systems has been an object of study since the 60 s, with the seminal work by Bretherton (Bretherton, 1961). Gas-liquid mass transfer has been also extensively studied. A comprehensive review of the topic was published by Haase and co-workers and the potential of Taylor flow reactors to boost the gas–liquid mass transfer of hydrophobic volatile organic contaminants at gas residence times of ~ 1 s has been recently proven (Kraakman et al., 2023). A more recent summary of different quantitative models of gas–liquid mass transfer rates can be found in an article by Abiev (Abiev, 2020). Fig. 6 of the last-mentioned article clearly showed the large discrepancies between the predictions of different models available in the literature. Despite the large discrepancies among models, all of them agree in considering the gas–liquid mass transfer from Taylor bubbles as being the result of two contributions, namely the transfer from the bubble hemispherical caps to the liquid slugs and the transfer from the bubble to the liquid film surrounding it. In order to solve the diffusion equations that govern both processes, it is necessary to obtain a solution of the Navier-Stokes equations describing the velocity field of the liquid in the mentioned regions (hemispherical caps and film around the bubbles). The fluid dynamics within the liquid slugs is qualitatively depicted in many works, but to our knowledge, no exact solution of the Navier-Stokes equations describing the fluid movement in the proximity of the hemispherical bubble caps has been obtained. The absence of such as solution makes that previous attempts to model gas–liquid mass transfer from the hemispherical caps (Van Baten and Krishna, 2004) are inspired by the solutions obtained from free rising bubbles, which are available at textbooks such as the one by Bird and co-workers (Bird et al., 2001). The liquid surrounding the bubbles follows the hydrodynamic of a falling liquid film (Thulasidas et al., 1995), which facilitates obtaining a solution for the diffusion problem.

In this work, an exact solution of the Navier-Stokes equation in the proximity of the hemispherical caps of Taylor bubbles, which allows obtaining also an exact solution of the mass transfer from the caps to the liquid slugs (the result is radically different from the free rising bubbles (Bird et al., 2001) was obtained. An exact solution of the gas–liquid mass transfer in the liquid film that separates the Taylor gas bubbles from the capillary walls is also presented (in the form of a Fourier Series). These results allow predicting mass transfer rates in Taylor flow reactors, without relying on experimentally adjusted parameters.

Functions predicting mass transfer coefficients are publicly available for the public in a Python library. This makes possible for scientists of any field to use them, without knowledge of CFD or any other specialized tools.

## 2. Methods

Taylor flow of gas–liquid mixtures is characterized by elongated gas bubbles rising within a capillary channel at a rate $U_b$. The gas bubbles can be seen as formed by two hemispherical caps and a cylindrical region. The cylindrical region of the gas bubble is separated from the walls of the capillary channel by a thin liquid film (Yue et al., 2009). The regions between gas bubbles are filled by liquid slugs. Far enough from the gas bubbles, the velocity distribution in these liquid slugs corresponds to a fully developed laminar flow in a cylindrical tube. Placing a system of reference in the rising gas bubbles (resting $U_b$ from all the velocities in the system), the bubbles can be seen as static with liquid flowing around them and moving from the upper to the lower slug through the film that separates the bubble from the wall. Choosing the rising gas bubbles as system of reference is fundamental to understand the mass transfer phenomena in Taylor flow reactors. The liquid slugs between gas bubbles, with the mentioned system of reference, can be seen as static regions in which the liquid rotates (upwards in the centre and downwards in the sides) flanked by a descending liquid film that carries the same liquid as the one that flows around the gas bubbles (Cherukumudi et al., 2015).

In this work, the Navier-Stokes equations in the liquid slugs above and under the hemispherical caps were first solved, which allowed to quantify the rate of mass transfer by convection and diffusion from the gas bubble to the upper and lower liquid slugs. Secondly, the diffusion equation in the liquid films that surrounds both the gas bubbles and the liquid slugs was solved. This allowed to quantify the total gas–liquid mass transfer rate.

### 2.1. Liquid velocity distribution in the neighbourhood of the hemispherical caps

The first step to quantify the rate of gas–liquid mass transfer in the hemispherical caps of Taylor flow gas bubbles, is to obtain a velocity distribution of the liquid above and below the bubbles. If one considers the liquid in the slugs between gas bubbles far enough from the bubble surfaces, this liquid is rising under a laminar flow regime (for values of the Reynolds number under 2000). For laminar flow in cylindrical capillaries of radius $R_c$, the fluid velocity is a function of the distance to the axis $R$.

$$u(R) = 2U_s\left[1 - \left(\frac{R}{R_c}\right)^2\right] \tag{1}$$

The parameter $U_s$ is the superficial slug velocity (the volumetric flow rate divided by the cross section of the capillary).

Now, instead of using the walls of the capillary as a system of reference, the Taylor gas bubbles can be used, which are rising at a rate $U_b$. In this new system of reference, the liquid velocity distribution in the slugs is the following:

$$u(R) = 2U_s\left[1-\left(\frac{R}{R_c}\right)^2\right] - U_b \tag{2}$$

The bubble caps can be considered to be, approximately, semi-spheres of radius $R_F$ and $R_B$ (in the forward and backward sides of the gas bubble, respectively). Both radii can be calculated using the following equations (Yue et al., 2009).

$$R_F = \frac{R_C}{1+1.286(3Ca)^{2/3}} \tag{3}$$

$$R_B = \frac{R_C}{1-0.464(3Ca)^{2/3}} \tag{4}$$

The capillarity number Ca depends on the bubble rising rate $U_b$ as follows:

$$Ca = \frac{\mu U_b}{\sigma} \tag{5}$$

With μ and σ being the liquid viscosity and liquid surface tension, respectively.

In spherical coordinates, the liquid velocity in the slugs between bubbles will have these two components:

$$u_\theta = -\left[2U_s\left[1-\left(\frac{rsin\theta}{R_s}\right)^2\right] - U_b\right]sin\theta \tag{6}$$

$$u_r = \left[2U_s\left[1-\left(\frac{rsin\theta}{R_s}\right)^2\right] - U_b\right]cos\theta \tag{7}$$

Velocity distributions with just two components can be described using the so-called stream function $\psi(r,\theta)$.

$$u_\theta = \frac{1}{rsin\theta}\frac{\partial\psi}{\partial r} \tag{8}$$

$$u_r = -\frac{1}{r^2 sin\theta}\frac{\partial\psi}{\partial\theta} \tag{9}$$

The stream function that corresponds to the velocity components represented in Equations (6) and (7) is:

$$\psi(r,\theta) = -\frac{2U_s - U_b}{2}r^2 sin^2\theta + \frac{1}{2}\frac{U_s}{R_c^2}r^4 sin^4\theta \tag{10}$$

This velocity distribution corresponds to a fully developed laminar flow that is not affected by the presence of the Taylor flow gas bubbles. Therefore, it is needed to obtain a stream function that tends asymptotically to Equation (10) for big distances from the bubble surface. This stream function must satisfy the Navier-Stokes equations with no acceleration (creeping flow). After applying the rotational operator ($\nabla\times$) to the velocity field, and expressing all the velocities in terms of the stream function, the Navier-Stokes equations for creeping flow can be compactly written as:

$$E^4\psi = 0 \tag{11}$$

Being the operator $E^2$:

$$E^2 = \left[\frac{\partial^2}{\partial r^2} + \frac{sinsin\theta}{r^2}\frac{\partial}{\partial\theta}\left(\frac{1}{sin\theta}\frac{\partial}{\partial\theta}\right)\right] \tag{12}$$

A stream function with the general form is proposed:

$$\psi(r,\theta) = (f_1(r) + g(r))sin^2\theta + f_2(r)sin^4\theta \tag{13}$$

The reason for introducing a separate term g(r) will become apparent later.

$$E^2\psi(r,\theta) = \left(\frac{d^2(f_1+g)}{dr^2} - \frac{2(f_1+g)}{r^2} + \frac{8f_2}{r^2}\right)sin^2\theta + \left(\frac{d^2f_2}{dr^2} - \frac{12f_2}{r^2}\right)sin^4\theta \tag{14}$$

$$E^4\psi(r,\theta) = \left(\frac{d^2}{dr^2}\left(\frac{d^2(f_1+g)}{dr^2} - \frac{2(f_1+g)}{r^2} + \frac{8f_2}{r^2}\right) - \frac{2}{r^2}\left(\frac{d^2(f_1+g)}{dr^2} - \frac{2(f_1+g)}{r^2} + \frac{8f_2}{r^2}\right) + \frac{8}{r^2}\left(\frac{d^2f_2}{dr^2} - \frac{12f_2}{r^2}\right)\right)sin^2\theta + \left(\frac{d^2}{dr^2}\left(\frac{d^2f_2}{dr^2} - \frac{12f_2}{r^2}\right) - \frac{12}{r^2}\left(\frac{d^2f_2}{dr^2} - \frac{12f_2}{r^2}\right)\right)sin^4\theta \tag{15}$$

Both terms multiplying the square and the fourth power of the sinus, have to be equal to zero. For the second term to be equal to zero, $f_2(r)$ has to take the following form:

$$f_2(r) = \frac{b_1}{r^3} + \frac{b_2}{r} + b_3 r^4 \tag{16}$$

To tend asymptotically to Equation (10), the parameter $b_3$ has to take the following form:

$$b_3 = \frac{1}{2}\frac{U_s}{R_c^2} \tag{17}$$

If Equation (16) is substituted in the term that multiplies sin2θ in Equation (15), the following expression is obtained:

$$\frac{d^2}{dr^2}\left(\frac{d^2(f_1+g)}{dr^2} - \frac{2(f_1+g)}{r^2} + \frac{8f_2}{r^2}\right) - \frac{2}{r^2}\left(\frac{d^2(f_1+g)}{dr^2} - \frac{2(f_1+g)}{r^2} + \frac{8f_2}{r^2}\right) + \frac{8}{r^2}\left(\frac{d^2f_2}{dr^2} - \frac{12f_2}{r^2}\right) = \left[\frac{d^2}{dr^2}\left(\frac{d^2f_1}{dr^2} - \frac{2f_1}{r^2}\right) - \frac{2}{r^2}\left(\frac{d^2f_1}{dr^2} - \frac{2f_1}{r^2}\right)\right] + \left[\frac{d^2}{dr^2}\left(\frac{d^2g}{dr^2} - \frac{2g}{r^2}\right) - \frac{2}{r^2}\left(\frac{d^2g}{dr^2} - \frac{2g}{r^2}\right)\right] + 224\frac{b_1}{r^7} \tag{18}$$

The function g(r) can be selected in order to satisfy the condition:

$$\left[\frac{d^2}{dr^2}\left(\frac{d^2g}{dr^2} - \frac{2g}{r^2}\right) - \frac{2}{r^2}\left(\frac{d^2g}{dr^2} - \frac{2g}{r^2}\right)\right] + 224\frac{b_1}{r^7} = 0 \tag{19}$$

Equation (19) has the solution:

$$g(r) = -\frac{4}{5}\frac{b_1}{r^3} \tag{20}$$

With this choice of g(r), the Navier-Stokes equations require that:

$$\left[\frac{d^2}{dr^2}\left(\frac{d^2f_1}{dr^2} - \frac{2f_1}{r^2}\right) - \frac{2}{r^2}\left(\frac{d^2f_1}{dr^2} - \frac{2f_1}{r^2}\right)\right] = 0 \tag{21}$$

Equation (21) is the same that appears in the problem of creeping flow around a spherical bubble and it has the general solution:

$$f_1(r) = \frac{a_1}{r} + a_2 r + a_3 r^2 \tag{22}$$

The asymptotic condition expressed in Equation (10) allows identifying the last parameter:

$$a_3 = -\frac{2U_S - U_b}{2} \tag{23}$$

The stream function describing the liquid velocity between Taylor flow gas bubbles will thus take the general form:

$$\psi(r,\theta) = \left(\frac{a_1}{r} + a_2 r - \frac{2U_s - U_b}{2}r^2 - \frac{4}{5}\frac{b_1}{r^3}\right)sin^2\theta + \left(\frac{b_1}{r^3} + \frac{b_2}{r} + \frac{1}{2}\frac{U_s}{R_c^2}r^4\right)sin^4\theta \tag{24}$$

The remaining parameters can be calculated from the boundary conditions in the gas–liquid interface. In the forward side of the bubble r = RF, these conditions are:

$$u_r(R_F) = 0 \tag{25}$$

$$\left(\frac{\partial u_\theta}{\partial r}\right)_{r=R_F} = 0 \tag{26}$$

In order to satisfy both boundary conditions, the parameters in Equation (24) take the following values:

$$b_1 = -\frac{5}{24}\frac{R_F^7}{R_c^2}U_s \tag{27}$$

$$b_2 = -\frac{7}{24}\frac{R_F^5}{R_c^2}U_s \tag{28}$$

$$a_1 = \frac{2U_s - U_b}{8}R_F^3 - \frac{2}{3}\frac{R_F^5}{R_c^2}U_s \tag{29}$$

$$a_2 = \frac{3(2U_s - U_b)}{8}R_F + \frac{1}{2}\frac{R_F^3}{R_c^2}U_s \tag{30}$$

These results allow calculating the fluid velocity in the surface of the gas bubble, which is necessary to quantify the gas–liquid mass transfer rate.

$$u_\theta(R_F,\theta) = \left(-\frac{3}{4}(2U_s - U_b) + \frac{2}{3}\frac{R_F^2}{R_c^2}U_s\right)sin\theta + \frac{35}{12}\frac{R_F^2}{R_c^2}U_s sin^3\theta \tag{31}$$

The fluid velocity becomes zero at the top of the gas bubble θ = 0 and at a critical angle θc:

$$sin\theta_c = \sqrt{\frac{\frac{3}{4}(2U_s - U_b) - \frac{2}{3}\frac{R_F^2}{R_c^2}U_s}{\frac{35}{12}\frac{R_F^2}{R_c^2}U_s}} \tag{32}$$

For angles smaller than the critical angle, the liquid circulates towards the centre of the gas bubble. This liquid remains in the slugs between gas bubbles. For angles larger than the critical one, the liquid flows around the gas bubbles and gets into the thin film that is formed between the bubbles and the wall of the capillary. Fig. 1 shows the stream lines predicted by the model.

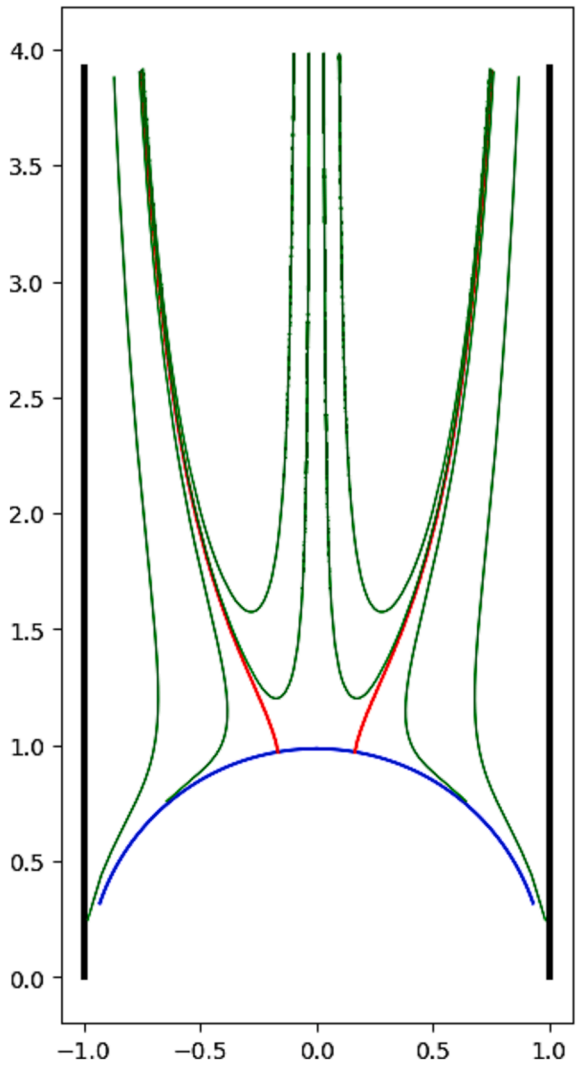


**Fig. 1.** Depiction of the stream lines that describe the liquid flow in the proximity of Taylor bubbles in a capillary channel of radius Rc = 1 mm with an average flow velocity Us = 0.1 m/s. The blue line depicts the bubble surface, the red lines show the stream lines that divide the liquid flowing around the bubbles from the liquid circulating within the liquid slugs. Green lines are stream lines parallel to the flow direction. The scale is shown in millimetres.

### 2.2. Gas-Liquid mass transfer from the hemispherical caps to the liquid slugs

The diffusion equation that governs the gas–liquid mass transfer in spherical coordinates (assuming that the diffusion term in the θ coordinate is negligible compared to the convection term), takes the following form:

$$u_\theta\frac{1}{r}\frac{\partial c}{\partial \theta} + u_r\frac{\partial c}{\partial r} = D\frac{\partial^2 c}{\partial r^2} \tag{33}$$

The parameter D is the diffusivity coefficient.

This equation will be solved using the same methodology that has been used for diffusion in spherical gas bubbles (Bird et al., 2001). First, the radial velocity, which is zero for r = RF, will be approximated by a linear relationship:

$$u_r = -\gamma\Delta r \tag{34}$$

In the previous equation, -γ is the partial derivative of $u_r$ at the gas bubble surface and Δr is the distance to the gas bubble surface.

The continuity equation in spherical coordinates determines the following relation, which can be used to correlate the parameter γ to the liquid velocity on the gas bubble surface:

$$\frac{\partial u_r}{\partial r} = -\frac{1}{rsin\theta}\frac{\partial}{\partial\theta}(u_\theta sin\theta) \tag{35}$$

The boundary conditions to solve Equation (33) are the following ones:

For $r = R_F$; $c = c_{eq}$.

For $r\to\infty$; $c = c_0$.

At the gas bubble surface, the concentration of the diffused species is equal to the concentration equilibrium with the gas ($c_{eq}$). Far away from the surface, the concentration tends to the bulk concentration of the liquid slug ($c_0$). It is convenient to define the following dimensionless concentration:

$$f = \frac{c - c_0}{c_{eq} - c_0} \tag{36}$$

The boundary conditions of the problem are: For r = $R_F$; f = 1; For $r\to\infty$; f = 0

#### 2.2.1. Mass transfer in the upper cap

At the critical angle θc, the upper cap of the bubble encounters a liquid stream perpendicular to the surface, which will be assumed to

have the concentration of the bulk concentration of the liquid slug. Thus, an extra boundary condition can be imposed:

For $\theta = \theta_c$; $f = 0$.

To transform Equation (33), from an equation in partial derivatives, into an ordinary differential equation, the following dimensionless variable will be defined:

$$\eta = \frac{\Delta r}{\delta(\theta)} \tag{37}$$

The function δ(θ) has length dimensions and will be chosen in order to make the following equation solvable:

$$\frac{d^2f}{d\eta^2} + \eta\frac{df}{d\eta}\left[\frac{1}{D}\left(\frac{u_\theta}{R_F}\delta(\theta)\frac{d\delta(\theta)}{d\theta} + \gamma\delta(\theta)^2\right)\right] = 0 \tag{38}$$

If the term between brackets takes a constant value of 2, the solution of Equation (38) is known. Therefore, a function δ(θ), for which the following relation is satisfied needs to be found:

$$\frac{1}{D}\left(\frac{u_\theta}{R_F + \Delta r}\delta(\theta)\frac{d\delta(\theta)}{d\theta} + \frac{1}{(R_F)sin\theta}\frac{\partial(u_\theta sin\theta)}{\partial\theta}\delta(\theta)^2\right) = 2 \tag{39}$$

This equation can be rearranged as follows:

$$\delta(\theta)\frac{d\delta(\theta)}{d\theta} + \frac{1}{u_\theta sin\theta}\frac{\partial(u_\theta sin\theta)}{\partial\theta}\delta(\theta)^2 = \frac{2D(R_F)}{u_\theta} \tag{40}$$

$$\frac{1}{2}\frac{d\delta(\theta)^2}{d\theta} + \frac{\partial ln(u_\theta sin\theta)}{\partial\theta}\delta(\theta)^2 = \frac{2D(R_F)}{u_\theta} \tag{41}$$

$$\frac{d\delta(\theta)^2}{d\theta} + \frac{\partial ln(u_\theta sin\theta)^2}{\partial\theta}\delta(\theta)^2 = \frac{4D(R_F)}{u_\theta} \tag{42}$$

$$\frac{d\delta(\theta)^2}{d\theta} + \frac{1}{(u_\theta sin\theta)^2}\frac{\partial(u_\theta sin\theta)^2}{\partial\theta}\delta(\theta)^2 = \frac{4D(R_F)}{u_\theta} \tag{43}$$

$$(u_\theta sin\theta)^2\frac{d\delta(\theta)^2}{d\theta} + \frac{\partial(u_\theta sin\theta)^2}{\partial\theta}\delta(\theta)^2 = (u_\theta sin\theta)^2\frac{4D(R_F)}{u_\theta} \tag{44}$$

$$\frac{\partial}{\partial\theta}\left(\delta(\theta)^2u_\theta^2sin^2\theta\right) = 4D(R_F)u_\theta sin^2\theta \tag{45}$$

In the forward cap, the boundary condition δ(θc) = 0, which is equivalent to f = 0, is used. Thus, Equation (45) can be integrated as follows:

$$\delta(\theta)^2u_\theta^2sin^2\theta = 4D(R_F)\int_{\theta_c}^{\theta}u_\theta sin^2\theta d\theta \tag{46}$$

The value of $u_\theta$ at the gas bubble surface has already been calculated (Equation (31). For simplicity $u_\theta$ can be written as follows:

$$u_\theta = -Asin\theta + Bsin^3\theta \tag{47}$$

With:

$$A = \frac{3}{4}(2U_s - U_b) - \frac{2}{3}\frac{R_F^2}{R_c^2}U_s \tag{48}$$

$$B = \frac{35}{12}\frac{R_F^2}{R_c^2}U_s \tag{49}$$

The integral in Equation (46) has the following solution:

$\int_{\theta_c}^{\theta}u_\theta sin^2\theta d\theta = -A\left[\frac{1}{3}cos^3\theta - cos\theta - \frac{1}{3}cos^3\theta_c + cos\theta_c\right] + B\left[-\frac{1}{5}cos^5\theta + \frac{2}{3}cos^3\theta - cos\theta + \frac{1}{5}cos^5\theta_c - \frac{2}{3}cos^3\theta_c + cos\theta_c\right]$‘ (50).

Using the function:

$$F(\theta) = (A-B)cos\theta + \left(\frac{2}{3}B - \frac{1}{3}A\right)cos^3\theta - \frac{1}{5}Bcos^5\theta \tag{51}$$

The function δ(θ) can be written as follows:

$$\delta(\theta) = \frac{1}{u_\theta sin\theta}\sqrt{4DR_F(F(\theta) - F(\theta_c))} \tag{52}$$

For this choice of δ(θ), Equation (38) has the solution:

$$f = 1 - \frac{2}{\sqrt{\pi}}\int_0^{\eta}e^{-\eta^2}d\eta \tag{53}$$

Using Fick's law, the flux density per unit of bubble surface will be equal to:

$$j = -D\left(\frac{\partial c}{\partial r}\right)_{r=R_F} = D(c_{eq} - c_0)\frac{2}{\sqrt{\pi}\delta(\theta)} \tag{54}$$

The total mass transfer across the forward bubble cap can be calculated from the integral:

$$J = 2\pi R_F^2\int_0^{\theta_c}jsin^2\theta d\theta \tag{55}$$

$$J = 2\sqrt{\pi DR_F^3}(c_{eq} - c_0)\int_0^{\theta_c}\frac{(-Asin\theta + Bsin^3\theta)sin^2\theta}{\sqrt{(F(\theta) - F(\theta_c))}}d\theta \tag{56}$$

With the following change of variable cosθ = x, the integral gets transformed as follows:

$$\int_0^{\theta_c}\frac{(-Asin^2\theta + Bsin^4\theta)sin\theta}{\sqrt{(F(\theta) - F(\theta_c))}}d\theta = \int_{cos\theta_c}^{1}\frac{-A(1-x^2) + B(1-x^2)^2}{\sqrt{(A-B)x + \left(\frac{2}{3}B - \frac{1}{3}A\right)x^3 - \frac{1}{5}Bx^5 - F(\theta_c)}}dx \tag{57}$$

This integral can be solved using a second change of variable:

$$y(x) = (A-B)x + \left(\frac{2}{3}B - \frac{1}{3}A\right)x^3 - \frac{1}{5}Bx^5 - F(\theta_c) \tag{58}$$

It can be shown that:

$$\frac{dy}{dx} = A(1-x^2) - B(1-x^2)^2 \tag{59}$$

Which transforms the integral as follows:

$$\int_{cos\theta_c}^{1}\frac{-A(1-x^2) + B(1-x^2)^2}{\sqrt{(A-B)x + \left(\frac{2}{3}B - \frac{1}{3}A\right)x^3 - \frac{1}{5}Bx^5 - F(\theta_c)}}dx = \int_0^{y(1)}\frac{-dy}{\sqrt{y}} = -2\sqrt{y(1)} \tag{60}$$

The square root in the previous equation is taken to be negative, so that the mass transfer rate takes a positive value.

Equation (32) can be transformed as follows:

$$cos\theta_c = \sqrt{1 - \frac{A}{B}} \tag{61}$$

Substituting Equation (61) and evaluating $y(x)$ for $x = 1$ in Equation (58), the following expression is obtained:

$$y(1) = (A-B)\left[1 - \left(1 - \frac{A}{B}\right)^{1/2}\right] + \left(\frac{2}{3}B - \frac{1}{3}A\right)\left[1 - \left(1 - \frac{A}{B}\right)^{3/2}\right] - \frac{1}{5}B\left[1 - \left(1 - \frac{A}{B}\right)^{5/2}\right] \tag{62}$$

#### 2.2.2. Mass transfer in the lower cap

The same methodology used in the previous section can be employed to obtain the rate of mass transfer in the lower cap. $R_B$, given by Equation (4), should be used instead of $R_F$.

$$A = \frac{3}{2}(2U_s - U_b) - \frac{2}{3}\frac{R_B^2}{R_c^2}U_s \tag{63}$$

$$B = \frac{35}{12}\frac{R_B^2}{R_c^2}U_s \tag{64}$$

If the angle θ is considered to be zero in the lowest part of the bubble, the velocity uθ has now positive values, instead of negative as in the previous case:

$$u_\theta = Asin\theta - Bsin^3\theta \tag{65}$$

For the lower cap, the bubble encounters a liquid stream perpendicular to the surface at θ = 0, which will be assumed to have the concentration of the bulk concentration of the liquid slug. Thus, the boundary condition will be:

For $\theta = 0$; $f = 0$.

This leads to the following equations for the lower cap:

$$\delta(\theta)^2 u_\theta^2 sin^2\theta = 4D(R_B)\int_0^\theta u_\theta sin^2\theta d\theta \tag{66}$$

$$\int_0^\theta u_\theta sin^2\theta d\theta = F(0) - F(\theta) \tag{67}$$

With the function $F$ defined in the same way as in Equation (51).

$$J = 2\sqrt{\pi D R_B^3}(c_{eq} - c_0)\int_0^{\theta_c}\frac{(Asin\theta - Bsin^3\theta)sin^2\theta}{\sqrt{(F(0) - F(\theta))}}d\theta \tag{68}$$

$$\int_0^{\theta_c}\frac{(Asin^2\theta - Bsin^4\theta)sin\theta}{\sqrt{F(0) - F(\theta)}}d\theta = \int_{cos\theta_c}^1 \frac{A(1-x^2) - B(1-x^2)^2}{\sqrt{F(0) - (A-B)x - \left(\frac{2}{3}B - \frac{1}{3}A\right)x^3 + \frac{1}{5}Bx^5}}dx \tag{69}$$

With the change of variable:

$$y = F(0) - (A-B)x - \left(\frac{2}{3}B - \frac{1}{3}A\right)x^3 + \frac{1}{5}Bx^5 \tag{70}$$

$$\int_{cos\theta_c}^1 \frac{A(1-x^2) - B(1-x^2)^2}{\sqrt{F(0) - (A-B)x - \left(\frac{2}{3}B - \frac{1}{3}A\right)x^3 + \frac{1}{5}Bx^5}}dx = \int_{y(cos\theta_c)}^0 \frac{-dy}{\sqrt{y}} = 2\sqrt{y(cos\theta_c)} \tag{71}$$

Substituting Equation (71) and evaluating $y(x)$ for $x = cos\theta_c$ in Equation (58), the following expression is obtained:

$$y(cos\theta_c) = (A-B)\left[1 - \left(1 - \frac{A}{B}\right)^{1/2}\right] + \left(\frac{2}{3}B - \frac{1}{3}A\right)\left[1 - \left(1 - \frac{A}{B}\right)^{3/2}\right] - \frac{1}{5}B\left[1 - \left(1 - \frac{A}{B}\right)^{5/2}\right] \tag{72}$$

This leads to a totally analogue expression for both the upper and lower caps, the only difference being due to different curvatures in both sides of the gas bubble.

### 2.3. Gas-liquid mass transfer from Taylor flow gas bubbles to the surrounding liquid film

#### 2.3.1. Determination of the essential parameters

The thickness of the film in the gas bubble region, $\delta_b$, is the main parameter governing gas–liquid mass transfer, as it will be discussed in the next section. Thus, in order to model gas–liquid mass transfer in Taylor flow reactors, it is essential to understand the factors governing the thickness of this film.

To model the thickness of the film in the gas bubble region, the following assumptions will be made:

There is no shear force acting on the gas–liquid interface. This assumption is valid in the absence of tenso-active compounds, or in other words, for constant surface tension.

The pressure inside bubbles can be considered constant and the curvature of the gas bubble in the region in which the film is formed is also constant.

The solution of Navier-Stokes equation for a liquid film of thickness $\delta_b$ falling under the effect of gravity inside a capillary channel of radius $R_c$, leads to the following solution for the volumetric liquid flow in the film (Thulasidas et al., 1997):

$$Q_f = \frac{\pi\rho g R_c^4}{8\mu}\left[1 + 4\left(\frac{R_c - \delta_b}{R_c}\right)^4\left[\frac{3}{4} - ln\left(\frac{R_c - \delta_b}{R_c}\right) - \left(\frac{R_c - \delta_b}{R_c}\right)^{-2}\right]\right] \tag{73}$$

The radius of the capillary channel minus the film thickness is equal to the radius of the rising bubbles $R_b = R_c - \delta_b$.

The total volumetric flow crossing any section of the capillary channel is equal to the surface velocity multiplied by the cross section of the capillary channel. This value is constant along the whole capillary channel. Thus, it has to be equal to the gas flow carried by rising gas bubbles minus the liquid flow falling in the film:

$$U_s\pi R_c^2 = U_b\pi R_b^2 - Q_f \tag{74}$$

Combining Equations (73) and (74), the following relation can be obtained:

$$\left(\frac{U_b}{U_s}\right)\left(\frac{R_b}{R_c}\right)^2 - 1 = \frac{\rho g R_c^2}{8\mu U_s}\left[1 + 4\left(\frac{R_b}{R_c}\right)^2\left[\frac{3}{4} - ln\left(\frac{R_b}{R_c}\right) - \left(\frac{R_b}{R_c}\right)^{-2}\right]\right] \tag{75}$$

The previous expression shows that the ratio $R_b/R_c$ depends on the ratio $U_b/U_s$ and an adimensional number representing the ratio between gravitational and viscous forces. This number will be herein referred to as S.

$$S = \frac{\rho g R_c^2}{8\mu U_s} \tag{76}$$

It remains to determine the ratio between the velocity of the rising gas bubbles and the average surface velocity. In the seminal article by Bretherton (Bretherton, 1961) it was argued that this ratio is a function only of the capillarity number Ca, defined as follows:

$$Ca = \frac{\mu U_s}{\sigma} \tag{77}$$

The parameter σ being the surface tension of the liquid. The relation proposed by Bretherton was:

$$\frac{U_b}{U_s} = \frac{1}{1 - 1.29(3Ca)^{2/3}} \tag{78}$$

According to the mentioned author, this function is valid for values of the capillarity number up to 0.005.

This means that the ratio $R_b/R_c$, and thus the ratio between the film thickness and the radius of the capillary channel, is a function of both the capillarity number and the previously defined number S:

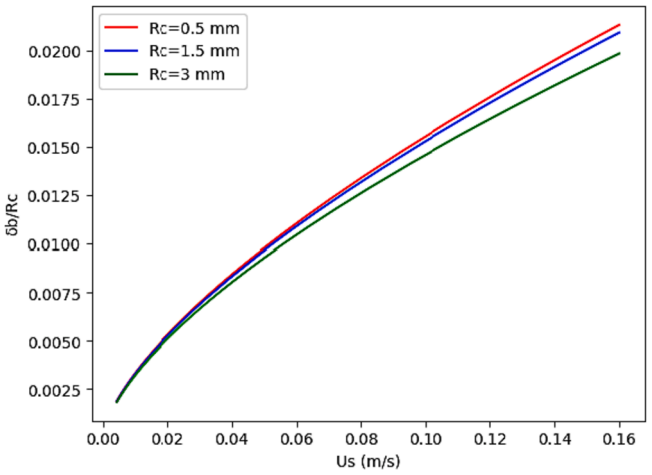


**Fig. 2.** Influence of the average velocity $U_s$ on the liquid film thickness for different radii of the capillary. Physical properties of pure water at 25 °C have been chosen.

$$\frac{\delta_b}{R_c} = 1 - \frac{R_b}{R_c} \tag{79}$$

Some authors have attempted to find correlations between the ratio $\delta_b/R_c$ and *Ca*. However, empirical determinations by Ausillous and Quéré (Ausillous and Quéré, 2000) show that the plots of $\delta_b/R_c$ versus *Ca* differ for different values of $R_c$. This divergence is explained by the fact that the number *S*, which depends on $R_c$, has also an impact on $\delta_b/R_c$. Fig. 2 shows how the thickness of the liquid film changes with the velocity of the bubbles.

As discussed previously, if the rising bubbles are considered as system of reference, the whole column can be seen as a series of bubbles separated by liquid slugs with a fluid film circulating around the bubbles and the slugs. It should be kept in mind that, in the region contacting the gas bubble, this film is moving downwards both in absolute terms and with respect to the gas bubble, while in the region contacting the slug, the film moves upwards in absolute terms but downwards with respect to the slug. Assuming a fully developed laminar flow in the central part of the slugs, the stream line that separates the liquid film along the liquid slug from the liquid slug is located at a distance $\delta_s$ from the wall, which, as it has been shown previously in reference (Thulasidas et al., 1997), takes the form:

$$\frac{R_c - \delta_s}{R_c} = \sqrt{2 - \frac{U_b}{U_s}} \tag{80}$$

The previous equation also can be obtained using the stream function that has been previously derived, by changing it to cylindrical coordinates and taking its asymptotic value at a large distance from the gas bubble surface.

### 2.3.2. Simulation of gas–liquid mass transfer in liquid films

In this section, whether the mass transfer from the gas bubbles to the surrounding liquid film is enough to saturate it, and whether the mass transfer to the liquid slug from the surrounding film is enough to equalize the film concentration with the slug concentration, was assessed. In the previous section it has been shown that, for any realistic operation condition, the thickness of the films δb and δs is small compared to the diameter of the capillary channel. Thus, in order to model gas diffusion, the films can be considered as flat.

With the purpose of determining the profile of concentration of the transferred chemical species in the liquid, the following differential equation needs to be solved:

$$u(y)\frac{\partial C(y,z)}{\partial z} = D\frac{\partial^2 C(y,z)}{\partial y^2} \tag{81}$$

With $u(y)$ being the velocity profile in the liquid film, $C(y,z)$ the gaseous substrate concentration in the liquid and *D* the diffusivity of the gaseous substrate in the liquid.

The variable z is the distance along the vertical axis. This axis will be considered as positive in the opposite sense to the bubble rise (the direction of flow of the liquid in the film relative to the bubble). The variable y is the distance from the wall of the capillary channel. The solutions of this equation have to satisfy the following boundary conditions:

$$C(\delta, z) = C_{eq} \tag{82}$$

$$C(y, 0) = C_{in} \tag{83}$$

$$\left(\frac{\partial C(y,z)}{\partial y}\right)_{y=0} = 0 \tag{84}$$

The first condition indicates the equilibrium at the gas–liquid interface (when dealing with the film surrounding the liquid slugs, this concentration is the concentration in the slug), and the second one represents an initial concentration at the beginning of the film. The third condition indicates that there is no gas flow across the capillary wall.

The problem can be simplified with the following change of variable:

$$C^*(y,z) = C(y,z) - C_{in} \tag{85}$$

Which would transform the boundary conditions as follows:

$$C^*(\delta, z) = C_{eq} - C_{in} = \Delta C \tag{86}$$

$$C^*(y, 0) = 0 \tag{87}$$

For simplicity, in the following equations Cin will be considered as zero. The conclusions can be easily extrapolated to other values.

A solution in the form of a Fourier series of cosines is herein proposed. The function is defined as a symmetric function in the interval $[-2\delta, 2\delta]$. Note that we are only interested in the form that the solution takes in the interval $[0, \delta]$, however the choice of using a Fourier series defined in the interval $[-2\delta, 2\delta]$ allows the boundary conditions in Equations (82) and (84) to be satisfied simultaneously. The solution proposed takes the following form:

$$C^*(y,z) = \Delta C - \sum_{n=1}^{\infty} a_n(z)\cos(\lambda_n y) \tag{88}$$

Where:

$$\lambda_n = \frac{n\pi}{2\delta} \tag{89}$$

The parameter $\delta$ is the thickness of the film, either in the gas bubble or slug region ($\delta_b$ or $\delta_s$ respectively).

In order to satisfy all the boundary conditions, the coefficients $a_n(z)$ should be chosen so that the summation $\sum_{n=1}^{\infty} a_n(0)\cos(\lambda_n y)$ converges to a value of $\Delta C$ in the interval $(-\delta, \delta)$ converges to zero at $y = \delta$ and $y = -\delta$ and to –ΔC in the intervals $[-2\delta, -\delta)$ and $(\delta, 2\delta]$.

A Fourier series of cosines is defined, which, in the interval $[0, 2\delta]$, will be equal to the liquid velocity profile:

$$u(y) = c_0 + \sum_{n=1}^{\infty} c_n \cos(\lambda_n y) \tag{90}$$

$$c_0 = \frac{1}{2\delta}\int_0^{2\delta} u(y)dy \tag{91}$$

$$c_n = \frac{1}{\delta}\int_0^{2\delta} u(y)\cos(\lambda_n y)dy \tag{92}$$

The reference system used in the simulation considers the bubble to have a zero velocity and the liquid is considered to be flowing along the z-axis in the positive direction. Solving the Navier-Stokes equations for a free-falling flat film (and adding the bubble velocity to take into account the system of reference) the following equation can be obtained:

$$u(y) = U_b + \frac{\rho g}{\mu}\left(\delta_b y - \frac{y^2}{2}\right) \tag{93}$$

The Fourier coefficients for this function are:

$$c_{b,0} = U_b + \frac{\rho g}{3\mu}\delta_b^2 \tag{94}$$

$$c_{b,n} = -\frac{\rho g}{\mu}\left(\frac{2\delta_b}{n\pi}\right)^2 (1 + cos(n\pi)) \tag{95}$$

In the region of a fully developed liquid slug, the velocity profile corresponds to the laminar flow in a cylinder. In this case, the liquid flows in the same direction as the bubbles move, which entails a negative sign.

$$u(y) = U_b - 2U_S\left(1 - \left(\frac{R_c - y}{R_c}\right)^2\right) \tag{96}$$

Its Fourier coefficients are:

$$c_{s,0} = U_b - 4U_s\frac{\delta_s}{R_c} + \frac{8}{3}U_s\left(\frac{\delta_s}{R_c}\right)^2 \tag{97}$$

$$c_{s,n} = -2U_s\left(\frac{2}{R_c}\left(\frac{2\delta_s}{n\pi}\right)^2\frac{1}{\delta_s}[cos(n\pi) - 1] - \frac{4}{R_c^2}\left(\frac{2\delta_s}{n\pi}\right)^2 cos(n\pi)\right) \tag{98}$$

After substituting the velocity and concentration by their Fourier expressions, the differential equation gets transformed as follows:

$$-\left(\sum_{n=0}^{\infty} c_n cos(\lambda_n y)\right)\left(\sum_{n=1}^{\infty} a_n'(z) cos(\lambda_n y)\right) = D\left(\sum_{n=1}^{\infty}\lambda_n^2 a_n(z) cos(\lambda_n y)\right) \tag{99}$$

The product of two Fourier series in the first term takes the form of a convolution:

$$-\sum_{n=1}^{\infty}\left(\sum_{m=0}^{n} c_m a'_{(n-m)}(z)\right) cos(\lambda_n y) = D\left(\sum_{n=1}^{\infty}\lambda_n^2 a_n(z) cos(\lambda_n y)\right) \tag{100}$$

Matching the coefficients of each cosine series, Equation (101) is obtained:

$$\lambda_n^2 D a_n(z) = -\sum_{m=0}^{n} c_m a'_{(n-m)}(z) \tag{101}$$

A solution for each $a_n(z)$ can be found recursively. The solution for n = 1 is:

$$a_1(z) = a_1(0)e^{-\frac{D}{c_0}\lambda_1^2 z} \tag{102}$$

Then, $a_n(z)$ can be calculated once the previous coefficients are known by solving the following differential equation:

$$a_n'(z) = -\sum_{m=1}^{n}\frac{c_m}{c_0} a'_{(n-m)}(z) - \frac{D}{c_0}\lambda_n^2 a_n(z) \tag{103}$$

In order to solve this equation, a solution in the form of a summation of exponentials is assumed:

$$a_n(z) = \sum_{i=1}^{n} K_{n,i} e^{-\alpha_i z} \tag{104}$$

The coefficients $K_{n,I}$ are marked with two sub-indexes, where $n$ indicates the Fourier coefficient and $i$ the position within the summation. For example $K_{1,1} = a_1(0)$. The exponents $\alpha_i$ take the form:

$$\alpha_i = \frac{D}{c_0}\lambda_i^2 \tag{105}$$

With the coefficients $\lambda_i$ defined as in Equation (89).

If all the Fourier coefficients are known from 1 to n-1, the summation that appears in the second term of Equation (103) can be calculated as follows:

$$-\sum_{m=1}^{n}\frac{c_m}{c_0} a'_{(n-m)}(z) = \sum_{m=1}^{n}\frac{c_m}{c_0}\sum_{i=1}^{n-m} K_{(n-m),i}\alpha_i e^{-\alpha_i z} \tag{106}$$

The second term can be rearranged as follows:

$$-\sum_{m=1}^{n}\frac{c_m}{c_0} a'_{(n-m)}(z) = \sum_{i=1}^{n-1}\alpha_i e^{-\alpha_i z}\sum_{m=1}^{n-i}\frac{c_m}{c_0} K_{(n-m),i} \tag{107}$$

In a more compact way, this can be rewritten as:

$$-\sum_{m=1}^{n}\frac{c_m}{c_0} a'_{(n-m)}(z) = \sum_{i=1}^{n-1} A_{n,i} e^{-\alpha_i z} \tag{108}$$

Where the coefficients $A_{n,I}$ take the form:

$$A_{n,i} = \sum_{m=1}^{n-i}\frac{c_m}{c_0}\alpha_i K_{(n-m),i} \tag{109}$$

And Equation (103) takes the form:

$$a_n'(z) = \sum_{i=1}^{n-1} A_{n,i} e^{-\alpha_i z} - \frac{D}{c_0}\lambda_n^2 a_n(z) \tag{110}$$

Making use of the equality shown in Equation (105), the previous equation can be rewritten as:

$$a_n'(z) = \sum_{i=1}^{n-1} A_{n,i} e^{-\alpha_i z} - \alpha_n a_n(z) \tag{111}$$

And using the expression shown in Equation (104), the following expression is obtained:

$$a_n'(z) = \sum_{i=1}^{n-1} A_{n,i} e^{-\alpha_i z} - \alpha_n\left(\sum_{i=1}^{n-1} K_{n,i} e^{-\alpha_i z} + K_{n,n} e^{-\alpha_n z}\right) \tag{112}$$

On the other hand, deriving Equation (104) leads to the following result:

$$a_n'(z) = -\sum_{i=1}^{n-1}\alpha_i K_{n,i} e^{-\alpha_i z} - \alpha_n K_{n,n} e^{-\alpha_n z} \tag{113}$$

Comparing the coefficients of the exponential terms, Equation (114) is obtained:

$$\alpha_i K_{n,i} = A_{n,i} - \alpha_n K_{n,i} \tag{114}$$

$$K_{n,i} = \frac{A_{n,i}}{\alpha_n - \alpha_i} \tag{115}$$

The previous equation allows obtaining all the coefficients for i < n. $K_{n,n}$ can be obtained from the initial condition:

$$K_{n,n} = a_n(0) - \sum_{i=1}^{n-1} K_{n,i} \tag{116}$$

The values of $a_n(0)$ remain to be determined, which can be done by calculating the Fourier coefficients that appear in Equation (88) for z = 0.

These coefficients take the form:

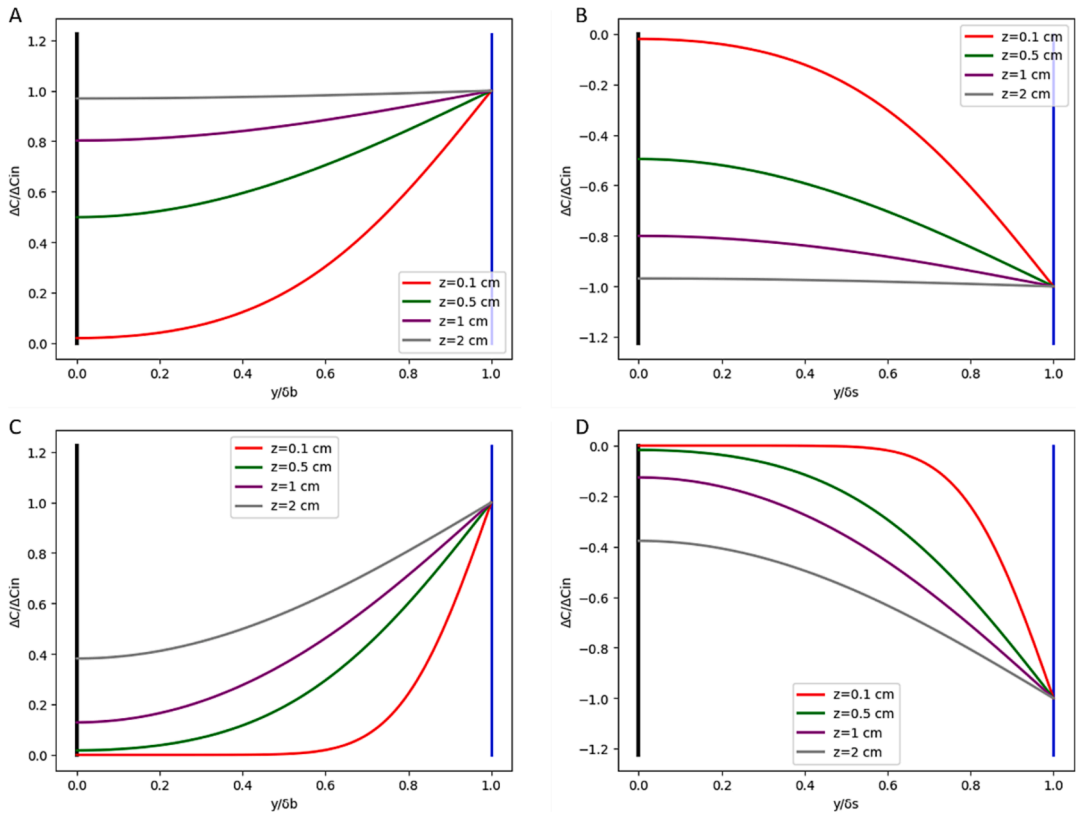


**Fig. 3.** Normalized concentration profiles of methane in water films around the bubbles (A and C) and around the slugs (B and D). Physical properties are taken at 25 °C and $R_c$ = 1 mm. The average velocity $U_s$ is 0.1 m/s (A and B) and 0.2 m/s (C and D).

$$a_n(0) = \frac{1}{\delta}\left(\int_0^{\delta} \Delta C cos(\lambda_n y)dy - \int_{\delta}^{2\delta} \Delta C cos(\lambda_n y)dy\right) = \Delta C \frac{4}{n\pi} \sin\left(\frac{n\pi}{2}\right) \tag{117}$$

Concentration profiles obtained solving the previous equations are depicted in Fig. 3.

Once the coefficients in Equation (88) have been determined and the concentration profiles calculated, it is possible to obtain the average concentration in the film after the contact with the bubble as follows:

$$\langle C(L_b)\rangle - C_{in} = \frac{1}{\delta_b}\int_0^{\delta_b} C^*(y, L_b)dy = \Delta C - \sum_{n=1}^{\infty} a_n(L_b)\left(\frac{2}{n\pi}\right) sin(\mathrm{n}\pi/2) \tag{118}$$

It should be noted that all the factors $a_n(z)$ are proportional to ΔC, thus it is possible define the following factor:

$$\varphi_b = \frac{\langle C(L_b)\rangle - C_{in}}{\Delta C} = 1 - \sum_{n=1}^{\infty} \frac{a_n(L_b)}{\Delta C}\left(\frac{2}{n\pi}\right) sin(\mathrm{n}\pi/2) \tag{119}$$

The factor φb is independent of ΔC. For long bubbles it tends to one, which means that the film around the bubble reaches the equilibrium concentration Ceq.

The same treatment as has been shown for the liquid film around the gas bubbles, can be used to describe the mass transfer in the film that surrounds the liquid slugs. If a homogeneous concentration $C_s$ is assumed within the slug, this will be the concentration at a distance $\delta_s$ from the wall. Thus, $C_{eq}$ will be substituted by $C_s$ and the difference $\Delta C$ will take negative values. In addition, the velocity profile within the film is the one expressed in Equation (96) and not the one in Equation (93). For the film surrounding the liquid slugs, a factor $\varphi_s$ can be defined:

$$\varphi_s = \frac{\langle C(L_s)\rangle - C_{in}}{\Delta C} \tag{120}$$

If $\varphi_s$ tends to one, the film reaches the concentration of the slug.

### 2.4. Quantification of the gas–liquid mass transfer in a complete Taylor flow reactor

In order to evaluate the gas–liquid mass transfer along the complete capillary column, a mass balance on a liquid slug will is carried out. There are three mass flows into each individual liquid slug, the diffusion from the upper bubble $J_B$, the diffusion from the lower bubble $J_F$, and the diffusion from the liquid film flowing downstream around the slug. For the sake of clarity, the coefficients $\varphi_b$ and $\varphi_s$ are initially taken as equal to one (the result will be generalized later). In this case, the fluid that circulates in the film is at equilibrium with the gas bubble when it gets in contact with the slug, and it reaches the concentration of the slug when it gets in contact with the next bubble. Thus, the mass transferred from the gas film to the slug is equal to the liquid flow in the film (relative to the bubbles and slugs), multiplied by the difference $(c_{eq} - c_s)$. The terms $J_B$ and $J_F$ are also proportional to $(c_{eq} - c_s)$, so it is convenient to rewrite them as $J_B = K_B(c_{eq} - c_s)$ and $J_F = K_F(c_{eq} - c_s)$. The mass balance on each individual liquid slug leads to the following differential equation:

$$V_s\frac{dC_s}{dt} = \left[K_B + K_F + Q_f + \pi U_b\left(2R_c\delta_b - \delta_b^2\right)\right]\left(C_{eq} - C_s\right) \tag{121}$$

For simplicity, all the terms between brackets were substituted by the symbol F. The previous differential equation can be rearranged as follows:

$$\frac{dC_s}{\left(C_s - C_{eq}\right)} = \frac{F}{V_s}dt \tag{122}$$

As a first approximation, the case of a pure gas will be considered, which allows taking $C_{eq}$ as a constant in the whole column.

The residence time of the slug in the column is equal to $L_c/U_b$, $L_c$ being the column length. Thus, the following solution for $C_s$ in the liquid outflow can be calculated:

$$C_s = C_{eq} - \left(C_{eq} - C_{s0}\right) e^{-\frac{F}{V_s}\frac{L_c}{U_b}} \tag{123}$$

At his point, it should be stressed that the ratio $F/V_s$ corresponds to what in the literature is known as $k_La$, even if such terminology is more appropriate for other types of mass transfer systems.

For shorter bubble or slug lengths, the coefficients $\varphi_b$ and $\varphi_s$ are smaller than one. In order to model this situation, the concentrations of two consecutive liquid slugs will be assumed to be almost identical and the average concentration in the liquid film at the end of the gas bubble will be considered the same as the average concentration in the film at the beginning of the slug (neglecting the effects of the region in which the gas bubble changes from a cylinder into a spherical cap). Similarly, the average concentration in the film at the beginning of the slug will be considered equal to the average concentration in the film at the end of the bubble. This allows us to use the following notation: $\langle C(L_b)\rangle = C_{si}$; $\langle C(L_s)\rangle = C_{bi}$. Therefore, the mass transfer from the film to the slug is not anymore $\left[Q_f + \pi U_b\left(2R_c\delta_b - \delta_b^2\right)\right]\left(C_{eq} - C_s\right)$ but $\left[Q_f + \pi U_b\left(2R_c\delta_b - \delta_b^2\right)\right]$ $\left(C_{si} - C_{bi}\right)$.

Making use of the coefficients $\varphi_b$ and $\varphi_s$, the following relations were established:

$$C_{eq} - C_{bi} = \frac{\left(C_{si} - C_{bi}\right)}{\varphi_b} \tag{124}$$

$$C_{si} - C_s = \frac{\left(C_{si} - C_{bi}\right)}{\varphi_s} \tag{125}$$

Adding the previous equations and rearranging them, Equation (126) was obtained:

$$C_{eq} - C_s = \left(\frac{1}{\varphi_b} + \frac{1}{\varphi_s} - 1\right)\left(C_{si} - C_{bi}\right) \tag{126}$$

Thus, the factor F that appears in Equation (122) can be expressed as:

$$F = K_B + K_F + \frac{Q_f + \pi U_b\left(2R_c\delta_b - \delta_b^2\right)}{\left(\frac{1}{\varphi_b} + \frac{1}{\varphi_s} - 1\right)} \tag{127}$$

Previously, the values $a_n(0)$ have been calculated assuming a constant concentration profile at the beginning of the film. This is valid when both factors $\varphi_b$ and $\varphi_s$ are close to one. If this is not the case, the problem can be solved by starting with a constant profile and obtaining $a_n(L_b)$, using this as an initial value to model the concentration profile in the film around the slug and obtain $a_n(L_s)$, and keep iterating until the obtained values for $\varphi_b$ and $\varphi_s$ stop changing significantly after each iteration.

## 3. Results

### 3.1. Comparison with experimental results from the literature

The predictions obtained using the equations derived in the previous section were compared with experimental results obtained by Bercic and Pintar for diffusion of pure methane in water (Bercic and Pintar, 1997). Bercic and Pintar report values of the $k_la$ for different operational conditions. For Taylor flow capillaries, this parameter is calculated experimentally from the inlet and outlet liquid concentrations using the following expression:

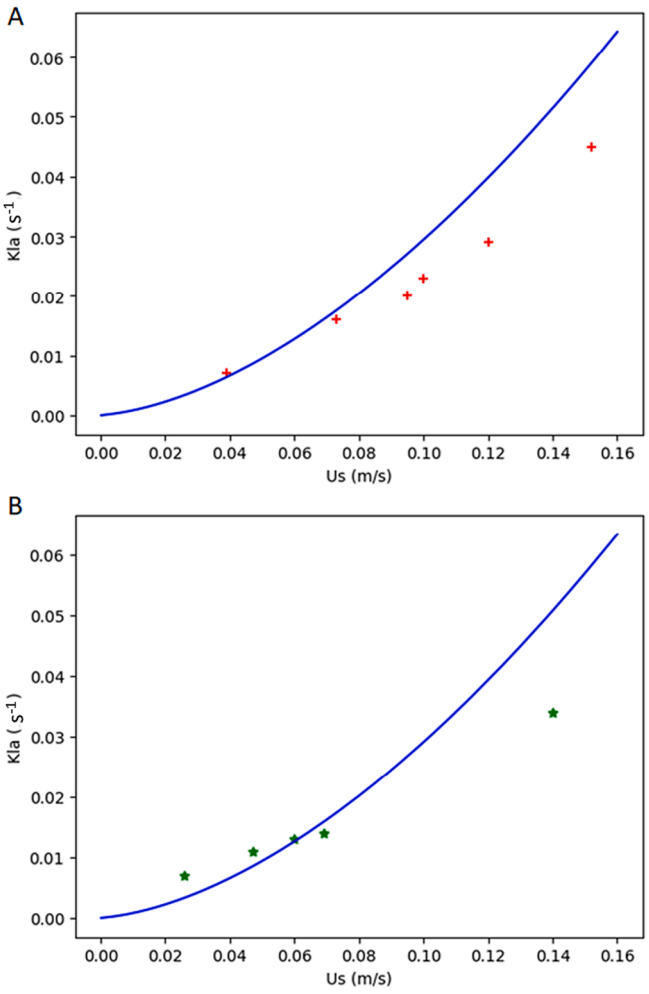


**Fig. 4.** Predicted and experimental dependence of the $k_La$ as a function of the average velocity $U_s$ for liquid slugs and bubble lengths $L_s = 11$ cm and $L_b = 11$ cm and capillary radii of 1.25 mm (A) and 1.55 mm (B). All the physical properties correspond to water and methane at 25 °C.

$$k_la = -\frac{U_b}{L_c} ln\left(\frac{C_{eq} - C_{out}}{C_{eq} - C_{in}}\right) \tag{128}$$

As it has been highlighted previously, for the case of diffusion of a pure gas, $k_la = F/V_s$. With $V_s$ equal to the volume of the liquid slugs.

A python library (pyTaylor) containing functions to compute this value (using the theoretical equations previously developed) can be found in the GitHub repository https://github.com/SergioBordel/Taylor.

The comparison between the $F/V_s$ predicted values and the experimental $k_la$ values reported in the literature are shown in Fig. 4.

### 3.2. Contributions to the total mass transfer

The function Kla in the library pyTaylor has two outputs, namely the contributions of the hemispherical caps and the liquid film. For every realistic situation, the contributions of the caps are two orders of magnitude lower than the contribution of the film (Fig. 5), so the gas–liquid mass transfer process under Taylor flow regime in capillaries is fully controlled by the thickness of the liquid film flowing around the Taylor gas bubbles.

As it can be seen in Fig. 5, the dependence of the film contribution on the average surface velocity is described by a concave function. This is due to the fact that the mass transfer rate increases with the velocity of

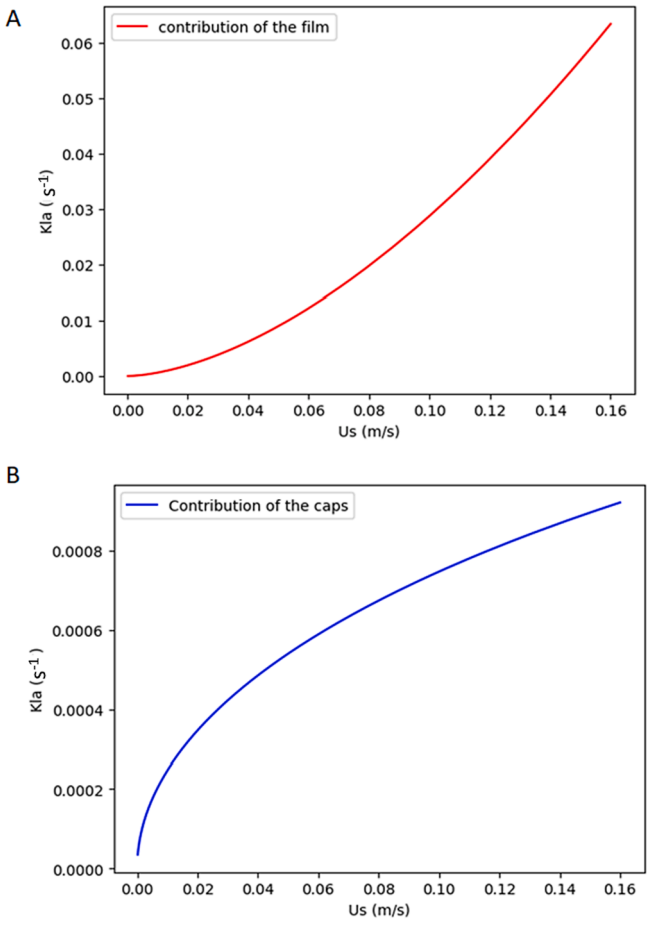


**Fig. 5.** Contributions of the liquid film and hemispherical caps to the total $k_La$ as a function of the average fluid velocity. The calculations have been carried out for liquid slugs and bubble lengths Ls = 11 cm and Lb = 11 cm and capillary radius of 1 mm. All the physical parameters are taken at 25 °C.

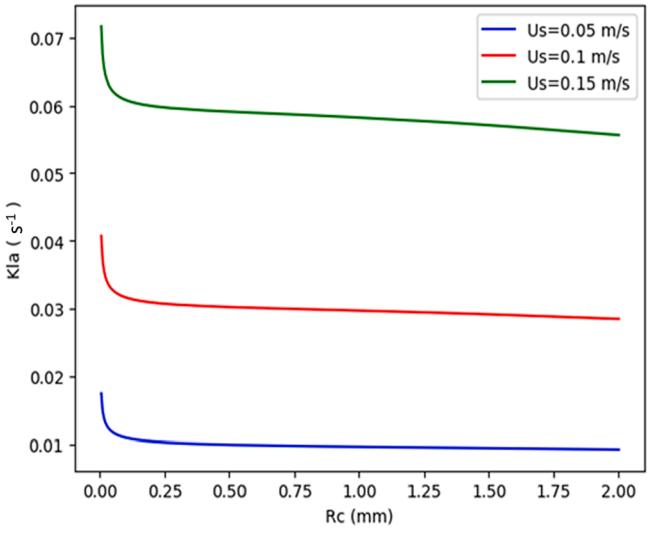


**Fig. 6.** Effect of the radius of the capillary channel on the mass transfer rate coefficient. The calculations have been carried out for liquid slugs and bubble lengths $L_s$ = 11 cm and $L_b$ = 11 cm and capillary channel radius up to 2 mm. All the physical parameters are taken at 25 °C.

the bubbles with respect to the surrounding fluid and the thickness of the surrounding liquid film (which also increases with the relative velocity of the bubbles with respect to the surrounding fluid). The contribution of the caps is described by a convex function, as it can be seen from equation (60), where the terms depending on the average surface velocity are within a square root.

Data from literature (Bercic and Pintar, 1997) have shown that the contribution of the radius $R_c$ to the gas–liquid mass transfer rate is almost negligible. In Fig. 6, the effect of the radius of the capillary has been computed for three different average velocities, which confirmed the minor effect of this operational parameter for $R_c$ above 0.1 mm.

### 3.3. *Effects of the bubble and slug lengths*

In most of the existing literature, the contributions to gas–liquid mass transfer of the bubble and slug lengths ($L_b$ and $L_s$) are not analysed separately. Instead, it is common to work with parameters such as the total unit length ($L_U$), which is the sum of both bubble and slug lengths, or the gas hold-up in the column (ε). Not taking account of the individual influences of $L_b$ and $L_s$, might be one of the reasons of the large discrepancies between the different models available in the literature (Abiev, 2020). Bergic and Pintar (Bercic and Pintar, 1997) did report the influence of bubble lengths, showing that for values between 11 and 2

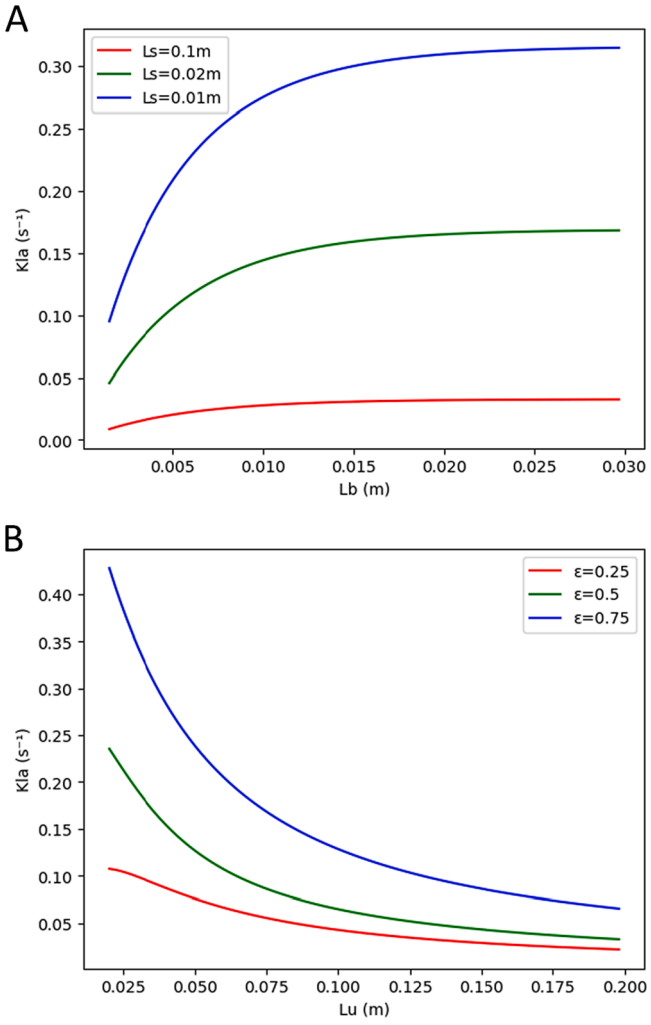


**Fig. 7.** Effect of the bubble length ($L_b$) and slug length ($L_s$) on the mass transfer coefficient (A). Effects of the unit length ($L_U$) and the gas hold-up (ε) on the mass transfer coefficient (B). The calculations have been carried out for $R_c$ = 1 mm and $U_S$ = 0.1 m/s. All the physical parameters are taken at 25 °C.

cm, no influence of the bubble length was observed. These authors interpreted such result as the contribution of mass-transfer to the liquid film being much lower than the transfer in the hemispherical caps. As it can be shown in Fig. 3, the reason for this observed lack of dependence on the bubble length, is not a low mass transfer from the gas bubbles to the surrounding liquid film, but the complete saturation of such film for bubbles longer than 2 cm. Regarding the influence of the length of the liquid slugs, Equation (123) shows that the $k_la$ is inversely proportional to the volume of the slug. This inverse relationship is confirmed by the experimental results reported by Bergic and Pintar (Bercic and Pintar, 1997). The dependence of the $k_la$ on the bubble and slug lengths (for a capillary radius of 1 mm and an average velocity of 0.1 m/s) are shown in Fig. 7. Knowing $L_b$ and $L_s$ it is possible to calculate the total unit length $L_U$ and the gas hold-up ε. The dependence of $k_la$ on these two parameters (more common in the literature) is also illustrated in Fig. 7.

### 3.4. Influence of physical parameters

So far, we have focused on the influence of operation parameters on the values of $k_la$. Here we explore the influence of viscosity and surface tension on the predicted values of $k_la$. Fig. 8 depicts the influence of viscosity for three different values of surface tension. Interestingly, the simulations show an optimal viscosity which decreases for lower surface tensions. For low viscosities, the mass transfer improves at lower surface tensions. For high viscosities the effect of the surface tension is the opposite.

### 3.5. Gas-liquid transfer of diluted compounds

Equation (123) has been obtained for the diffusion of a pure gas into the surrounding liquid. In this case the equilibrium concentration $C_{eq}$ remains constant along the gas column. This is the scenario corresponding to the experimental set-up used by Bergic and Pintar (Bercic and Pintar, 1997), in which pure methane was used. For many practical applications, the chemical species to be transferred is present at low concentrations in the gas phase and its concentration decreases as the gas bubbles rise in the column.

If we make the approximation of a small concentration difference between contiguous bubbles. We can establish the following mass balance:

$$V_s dC_s = -V_b dC_b \tag{129}$$

and

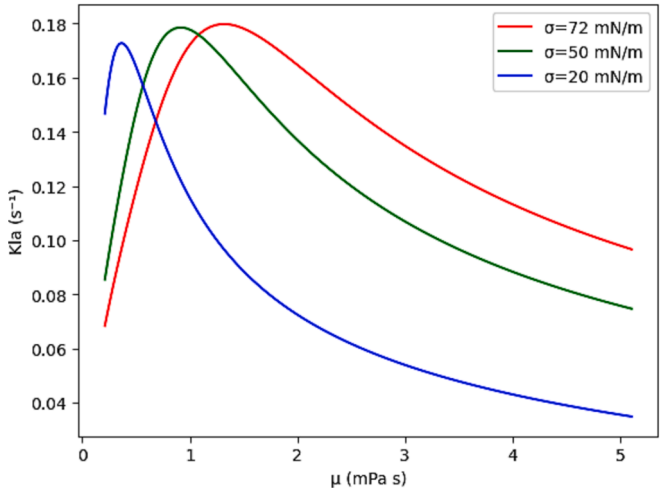


**Fig. 8.** Effect of viscosity and surface tension on the mass transfer coefficients. Calculations have been carried out for the following operation conditions: $U_s$ = 0.1 m/s; $R_c$ = 1 mm; $L_s$ = 2 cm; $L_b$ = 2 cm.

$$V_s \Delta C_s = -V_b \Delta C_b \tag{130}$$

The equilibrium concentration and the concentration in the bubble are related as follows:

$$C_{eq} = \frac{C_b}{m} \tag{131}$$

The parameter m is the non-dimensional Henry constant for the transferred compound.

The differential equation can now be solved using the following change of variable:

$$d(C_{eq} - C_s) = -\left(\frac{V_s}{mV_b} + 1\right) dC_s \tag{132}$$

Which leads to the following result for the liquid concentration at the column outlet:

$$C_s = C_{s0} + \frac{(C_{eq0} - C_{s0})}{1 + \frac{V_s}{mV_b}} \left(1 - e^{-F\left(\frac{1}{mV_b} + \frac{1}{V_s}\right)\frac{L_c}{U_b}}\right) \tag{133}$$

The outlet gas concentration will be:

$$C_{bout} = C_{b0} - \frac{V_s}{V_b} \frac{(C_{eq0} - C_{s0})}{1 + \frac{V_s}{mV_b}} \left(1 - e^{-F\left(\frac{1}{mV_b} + \frac{1}{V_s}\right)\frac{L_c}{U_b}}\right) \tag{134}$$

## 4. Discussion

After obtaining exact solutions for the Navier-Stokes equations and the diffusion equations, it is possible to conclude that the process of gas–liquid mass transfer in Taylor flow regime is essentially controlled by the mass transfer to the liquid film near the walls of the capillary channel. Interestingly, the contribution of the spherical caps is two orders of magnitude lower than the contribution of the film.

To the best of our knowledge, exact solutions of the equations governing gas–liquid mass transfer under Taylor flow, had not been obtained previously. Instead, in much of the available literature, the mass transfer from the hemispherical bubble caps to the liquid slugs, was modelling using the expression obtained for free rising bubbles (Bird et al., 2001), with some variations (Table 1). These expressions for the mass transfer in the caps, do not correspond to the actual hydrodynamics of Taylor flow and lead to large over-estimations of mass transfer.

Some authors (Bercic and Pintar, 1997) have suggested that most of the mass transfer occurs from the hemispherical caps, because the value of the $k_la$ did not seem to depend on the bubble length. This is due to the saturation of the film surrounding the gas bubbles, which makes that no further transfer occurs beyond a particular value of $L_b$.

## 5. Conclusions

The model presented here identified four independent operational parameters (besides the physical constants) affecting the $k_la$. These parameters are the average velocity $U_s$, the radius of the capillary $R_c$, and the lengths of the bubbles $L_b$ and liquid slugs $L_s$. The size of the liquid

**Table 1**

| Contribution of the caps to the $k_La$ | Reference |
|---|---|
| $k_L = \sqrt{\frac{4}{3\pi}\frac{Du_\infty}{2R_c}}$ | Free rising bubble (Bird et al., 2001) |
| $k_{L,cap} = 2\sqrt{2\frac{4}{\pi^2}\frac{DU_b}{R_c}}$ | Higbie penetration model (Abiev, 2020; Sherwood et al., 1975; López de León et al., 2023) |
| $a_{cap} = \sqrt{\frac{4}{L_{UC}}}$ | |

slugs is rarely reported in the experimental literature. The total unit length ($L_s + L_b$) or the gas hold up ε are more commonly reported, but the bubble length exerts a very weak impact on the transfer properties beyond a certain threshold, due to the saturation of the liquid film surrounding it, thus the total unit length can be not very informative. Similarly, the same gas hold up could be achieved by longer or shorter bubbles and liquid slugs, leading to very different mass transfer rates. The average velocity $U_s$ has a strong impact on the $k_la$. However, if Taylor flow reactors are designed to transfer as much gas as possible to the liquid phase, the model shows that large bubble velocities $U_b$ (with values always very close to $U_s$) have a negative impact on the mass transfer by decreasing the residence time of the gas bubbles in the capillary. The capillary radius $R_c$ has shown to have a very weak effect on $k_la$. The operational parameter with the largest influence on the transfer capabilities of the system was the volume of the liquid slugs (see Equation (123), which depends on the slug length $L_s$ and ultimately is determined by the mechanism of mixing the gas and liquid streams. The equations presented in this work could be useful to put in perspective the experimental results of mass transfer obtained in Taylor flows and guide in the scale up of this platform technology.

## CRediT authorship contribution statement

**Sergio Bordel:** Conceptualization, Data curation, Formal analysis, Methodology, Software, Writing – original draft, Writing – review & editing. **Norbertus J. R. Kraakman:** Conceptualization, Data curation, Writing – review & editing. **Raúl Muñoz:** Funding acquisition, Supervision, Writing – review & editing.

## Declaration of competing interest

The authors declare that they have no known competing financial interests or personal relationships that could have appeared to influence the work reported in this paper.

## Data availability

No data was used for the research described in the article.

## Acknowledgments

This work was supported by the Ministry of Science, Innovation and Universities [project RTI2018-0-096441-B-I00]. The Regional Government of Castilla y León and the EU-FEDER program [grant number CLU 2017-09, CL-EI-2021-07 and UIC 315] are also gratefully acknowledged.

## References

Abiev, R.S., 2020. Gas-liquid and gas-liquid-solid mass transfer model for Taylor flow in micro (milli) channels: a theoretical approach and experimental proof. Chem. Eng. J. Adv. 4, 100065 https://doi.org/10.1016/j.ceja.2020.100065.

Ausillous, P., Quéré, D., 2000. Quick deposition of a fluid on the wall of a tube. Phys. Fluids 12, 2367–2371.

Bercic, G., Pintar, A., 1997. The role of gas bubbles and liquid slug lengths on mass transport in the Taylor flow through capillaries. Chem. Eng. Sci 52, 3709–3719. https://doi.org/10.1016/S0009-2509(97)00217-0.

Bird, R.B., Stewart, W.E., Lightfoot, E.N., 2001. Transport phenomena. Wiley, New York, USA.

Bretherton, F.P., 1961. The motion of long bubbles in tubes. J. Fluid Mech. 10, 166–188. https://doi.org/10.1017/S0022112061000160.

Cherukumudi, A., Klaseboer, E., Khan, S.A., Manica, R., 2015. Prediction of the shape and pressure drop of Taylor bubbles in circular tubes. Microfluid. Nanofluid. 19, 1221–1233. https://doi.org/10.1007/s10404-015-1641-x.

EU Biorefinery Outlook to 2030. https://ec.europa.eu/info/news/eu-biorefinery-outlook-2030-2021-jun-02_en (last access 22/10/2022).

Gavala, H.N., Grimalt-Alemany, A., Asimakopoulos, K., Skiadas, I.V., 2021. Gas biological conversions: the potential of syngas and carbon dioxide as production platforms. Waste Biomass Valoriz. 12, 5303–5328. https://doi.org/10.1007/s12649-020-01332-7.

Haase, S., Murzin, D.Y., Salmi, T., 2016. Review on hydrodynamics and mass transfer in minichannel wall reactors with gas-liquid Taylor flow. Chem. Eng. Res. & Des. 113, 304–329. https://doi.org/10.1016/j.cherd.2016.06.017.

Harmsen, J.H.M., van Vuuren, D.P., Navak, D.R., Hof, A.F., Hoglund-Isaksson, L., Lucas, P.L., Nielsen, J.B., Smith, P., Stehfest, E., 2019. Long-term marginal abatement cost curves of non-CO2 greenhouse gases. Environmental Sciences and Policy. 99, 136–149.

Kraakman, N.J.R., Roche Rios, J., van Loosdrecht, M.C.M., 2011. Review of mass transfer aspects for biological gas treatment. Appl. Microbiol. Biotechnol. 91, 873–886.

Kraakman, N.J.R., González-Martína, J., Rodriguez, E., Lebrero, R., Deshusses, M.A., Muñoz, R., 2023. Hydrophobic air pollutants removal at one second gas contact in a multi-channel capillary bioreactor. J. of Environmental Chemical Engineering 11, 110502.

Kreutzer, M.T., Kapteijn, F., Moulijn, J.A., Heiszwolf, J.J., 2005. Multiphase monolith reactors: chemical reaction engineering of segmented flow in microchannels. Chem Eng Sci 60, 5895–5916.

López de León, R., Deaton, K.E., Deshusses, M.A., 2023. Modeling of a capillary microbioreactor for VOC removal. Chem. Eng. J. https://doi.org/10.1016/j.cej.2023.141636.

Nijhuis, T.A., Beers, A.E.W., Vergunst, T., Hoek, I., Kapteijn, F., Moulijn, J.A., 2001. Preparation of monolithic catalysts. Catalysis Reviews—Science and Engineering 43 (4), 345–380.

Shao, N., Gavriilidis, A., Angeli, P., 2009. Flow regimes for adiabatic gas-liquid flow in microchannels. Chem. Eng. Sci. 64, 2749–2761.

Sherwood, T.K., Pigford, R.L., Wilke, C.R., 1975. Mass transfer. Mc-Graw Hill, New York, USA.

Stone, K.A., Hilliard, M.V., He, Q.P., Wang, J., 2017. A mini review on bioreactor configurations and gas transfer enhancements for biochemical methane conversion. Biochem. Eng. J. 128, 83–92.

Thulasidas, T.C., Abraham, M.A., Cerro, R.L., 1995. Bubble-train flow in capillaries of circular and square cross section. Chem. Eng. Sci. 50 (2), 183–199. https://doi.org/10.1016/0009-2509(94)00225-G.

Thulasidas, T.C., Abraham, M.A., Cerro, R.L., 1997. Flow patterns in liquid slugs during bubble-train flow inside capillaries. Chem. Eng. Sci. 52 (17), 2947–2962. https://doi.org/10.1016/s0009-2509(97)00114-0.

Van Baten, J.M., Krishna, R., 2004. CFD simulations of mass transfer from Taylor bubbles rising in circular capillaries. Chem. Eng. Sci. 59 (12), 2535–2545. https://doi.org/10.1016/j.ces.2004.03.010.

Yue, J., Luo, L., Gonthier, Y., Chen, G., Yuan, Q., 2009. An experimental study of air–water Taylor flow and mass transfer inside square microchannels. Chem. Eng. Sci 64 (16), 3697–3708. https://doi.org/10.1016/j.ces.2009.05.026.